International Journal of Biological Macromolecules 269 (2024) 132186

Contents lists available at ScienceDirect

International Journal of Biological Macromolecules

journal homepage: www.elsevier.com/locate/ijbiomac

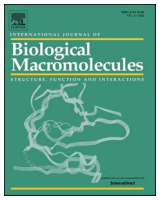

Fenugreek seed mucilage-based active edible films for extending fresh fruit shelf life: Antimicrobial and physicochemical properties

Ali Mohammadi Lindi [a], Leila Gorgani [a], Maedeh Mohammadi [a], Sepideh Hamedi [b], Ghasem Najafpour Darzi [a], Pierfrancesco Cerruti [c], Ehsan Fattahi [d], Arash Moeini [d,*]

[a] Biotechnology Research Laboratory, Faculty of Chemical Engineering, Babol Noshirvani University of Technology, 47148 Babol, Iran
[b] Department of Bio-refinery, Faculty of New Technologies Engineering, Shahid Beheshti University, Tehran, Iran
[c] Institute for Polymers, Composites and Biomaterials (IPCB) - CNR, Via Gaetano Previati, 1/E, 23900 Lecco, Italy
[d] Research Group of Fluid Dynamics, Chair of Brewing and Beverage Technology, TUM School of Life Sciences, Technical University of Munich, 85354 Freising, Germany

ARTICLE INFO

Keywords:
Edible coating
Fenugreek seed mucilage
Shelf life
Antimicrobial activity
Sustainable packaging

ABSTRACT

Trigonella foenum-graecum, known as fenugreek, belongs to the leguminous family of wild growth in Western Asia, Europe, the Mediterranean, and Asia; its ripe seeds contain a pool of bioactive substances with great potential in the food industry and medicine. In this study, fenugreek seed mucilage (FSM) was extracted and characterized in its structural properties by X-ray diffraction, nuclear magnetic resonance, and high-performance liquid chromatography. Then, the applicability of FSM as an antimicrobial agent was demonstrated via the development of novel, active, edible FSM-based biofilms containing carboxymethyl cellulose and rosemary essential oil (REO). Incorporating REO in the biofilms brought about specific changes in Fourier-transform infrared spectra, affecting thermal degradation behavior. Scanning electron microscopy and atomic force microscopy morphography showed an even distribution of REO and smoother surfaces in the loaded films. Besides, the solubility tests evidenced a reduction in water solubility with increasing REO concentration from 1 to 3 wt%. The biological assay evidenced the antimicrobial activity of REO-loaded biofilms against *Staphylococcus aureus* and *Escherichia coli*. Finally, whole apples were dip-coated with FSM-based solutions to showcase future edible systems. The REO-loaded biofilms extended the shelf life of apples to 30 days, demonstrating their potential for sustainable and active coatings.

1. Introduction

The primary functions of food packaging (FP) include protecting foodstuff, facilitating transportation, and enhancing user convenience. Besides, FP is crucial in preserving foodstuff quality and extending its shelf life. The ever-increasing use of FP has led to a sharp growth in the use of plastics in the food industry, raising concerns about its environmental impact. Consequently, there is a growing need to develop alternative packaging materials that are biodegradable and environmentally friendly [1]. Recently, there has been a surging inclination towards the development of biodegradable films produced from biopolymers, such as polysaccharides, lipids, proteins and their composites, due to their characteristics, such as biodegradability, renewability, and abundance [2,3]. Biodegradable films can even reduce microbial proliferation, improve food quality, and increase shelf life [4].

Trigonella foenum-graecum, known as fenugreek, is a leguminous plant that originated in Western Asia and has spread over Europe, the Mediterranean, and Asia [5]. The ripe seeds have several applications in traditional Indian herbal medicine, including the treatment of colic flatulence, dysentery, diarrhea, dyspepsia with loss of appetite, chronic cough, dropsy, liver and spleen enlargement, rickets, gout, and diabetes [5,6]. The green leaves and seeds of fenugreek have been used in the food industry as additives, flavoring agents, and preservatives, as well as in traditional medicine. Fenugreek seeds exhibit biological activities, including antidiabetic, anticancer, antioxidant, anti-inflammatory, antibacterial, gastric stimulant for anorexia, and hepatoprotective [7,8]. Fenugreek seeds contain a significant percentage of mucilage, a natural gummy material that coats many seeds to facilitate hydration and germination [7]. Mucilage is a biocompatible, non-toxic, low-cost hydrocolloid, mainly made of high molecular weight polysaccharides with a desirable film-forming ability [9]. It is broadly used in the food and pharmaceutical industries as a thickener, suspending agent, binder,

* Corresponding author.
E-mail address: arash.moeini@tum.de (A. Moeini).

https://doi.org/10.1016/j.ijbiomac.2024.132186
Received 19 March 2024; Received in revised form 26 April 2024; Accepted 6 May 2024
Available online 7 May 2024

and emulsion stabilizer [10]. Fenugreek seed mucilage (FSM) is mainly based on polysaccharides, with a crystalline structure containing 45–60 % carbohydrates, mostly fiber, 30 % soluble, and 20 % insoluble [11].

Fenugreek seeds, integral to various Indian recipes, are particularly rich in mucilage. While not highly soluble in water, FSM exhibits a thick consistency when dissolved, a property advantageous for film development. Exploring its application in edible films is of significant interest, especially considering its unique properties and potential benefits in the food industry. Furthermore, FSM exhibits impressive emulsifying properties, significantly enhancing dispersion in soy protein isolate and demonstrating stability across various pH levels and high temperatures [12]. Such characteristics highlight its versatility, not just as an ingredient in traditional cuisine but also in innovative food technology applications.

Carboxymethyl cellulose (CMC), an anionic and water-soluble polysaccharide, has emerged as a popular choice for the formulation of biofilms due to its affordability, non-toxicity, odorlessness, non-allergenic nature, thermal stability, and biodegradability [13,14]. However, pure CMC-based biofilms suffer from weak water resistance, limiting their effectiveness in packaging and preserving food products [13]. Blending CMC with other biodegradable polymers has been proposed to address this constraint and improve the inherent properties of CMC-based films for use in edible food packaging.

The latter can include antimicrobial agents, among which benzoates, propionates, parabens, sorbates, enzymes, bacteriocins, and essential oils, to control the microbial contamination of food products and extend their shelf life [15]. Essential oils are natural substances derived from plants developed as popular antibacterial and antioxidants in active packaging [16–18]. Incorporating essential oils into active packaging can enhance food products' shelf life by limiting spoilage microorganism growth and reducing food deterioration [19].

Rosmarinus officinalis (rosemary) essential oil (REO) is an effective antibacterial agent that contains various phenolic compounds, such as carnosol, carnosic, and rosmarinic acids, which play a pivotal role in its antioxidant and antimicrobial properties. The primary constituents of REO include α-pinene, camphor, 1,8 cineole, and bornyl acetate [20]. Notably, 1,8-cineole, when combined with a-pinene and/or terpinene-4-ol, exhibits a considerable synergistic effect on the penetration and damage of microbial cell membranes [21]. In the context of our study, the integration of REO into FSM-based films is hypothesized to enhance these films' antimicrobial efficacy, contributing to a novel approach in food packaging.

On the basis of the above considerations, herein we report the preparation of FSM-based active edible films containing CMC as a structural component and REO as an antimicrobial agent. To the best of our knowledge, this combination has yet to be reported. The effect of different concentrations of REO on the water solubility, water vapor permeability, light transmission, and mechanical properties of the prepared films was examined. The antibacterial features of the films against Gram-negative (*Escherichia coli*) and Gram-positive (*Staphylococcus aureus*) bacteria were also assessed. Finally, a proof-of-concept of their use in active food packaging is provided, evaluating the potential of the films in extending apple shelf life over a specific period.

2. Materials and methods

2.1. Materials

Fenugreek seeds were purchased from a local retail store (Mazandaran province, Iran). Rosemary essential oil (REO) extracted from *Salvia rosmarinus* was bought from Barij Essence Pharmaceutical Co. (Kashan, Iran). Folin-Ciocalteu reagent (FCR), glycerol, tween 80, carboxymethyl cellulose (CMC), 2,2-diphenyl-1-picrylhydrazyl (DPPH), trifluoracetic acid (TFA), and gallic acid were acquired from MilliporeSigma (Massachusetts, United States). Methanol and ethanol were obtained from Chemlab-Analytical (West Flanders, Belgium). Nutrient broth (NB) and nutrient agar (NA) were bought from QLAB (Canada). *Staphylococcus aureus* (*S. aureus* PTCC 1431) and *Escherichia coli* (*E. coli* PTCC 1330) were acquired from the Iranian Research Organization for Science and Technology (IROST; Tehran, Iran).

2.2. FSM extraction and analysis

According to our previous study, FSM was obtained through ultrasound-assisted extraction using a 1:55 mass ratio of solid to water as the solvent [22]. The mixture was positioned inside an ultrasound bath, set to operate at a power level of 100 W, a frequency of 37 kHz, and a temperature of 55 °C for 30 min. These extraction parameters were established according to initial experiments to achieve the maximum mucilage yield. Following the sonication procedure, the mixture underwent filtration using a cloth filter to separate the extracted mucilage from the seed biomass.

The extracted FSM's monosaccharide composition was verified using a high-performance liquid chromatography apparatus (HPLC) (Agilent 1220 Infinity Isocratic LC). First, a specific amount of FSM underwent hydrolysis at 120 °C for 3 h in a screw-capped vial utilizing 3 mL of TFA solution (2 M). Next, ethanol was added to remove the excess amounts of acid and repeated 5 times. A solution mixture of 1-phenyl-3-methyl-5-pyrazolone (0.5 M) and sodium hydroxide (0.6 M) was introduced to the dried hydrolysis product and then reacted for 2 h at 70 °C. Afterward, the resulting product was neutralized by adding 0.1 mL of hydrochloric acid solution and going through successive extractions using chloroform. The aqueous phase was passed through a 0.45 μm membrane filter and injected into the C18 column for HPLC analysis. A mixture of acetonitrile and phosphate buffer solution (0.1 M, pH = 7.6) was employed as the mobile phase in an 80:20 ratio, at a 1 mL/min flow rate.

^{13}C and ^{1}H nuclear magnetic resonance (NMR) spectra were acquired using a Bruker Advance 500 MHz spectrometer (Bruker, United States) at 125 and 500 MHz frequencies, respectively. D_2O was used as the solvent, and all experiments were performed at room temperature. The ^{13}C spectra were obtained with 100,000 scans and an acquisition time of 1.1 s, while the ^{1}H spectra were acquired with 64 scans and an acquisition time of 3.1 s. X-ray diffraction (XRD) characterization was performed on a Philips PW1730 diffractometer (Philips, Netherlands) with Cu Kα radiation to establish the FSM powder's crystalline phase and structure. For this purpose, dry FSM was finely ground using a rotary motion with a mortar and pestle to obtain particles, and the ground powder was poured onto the sample holder.

2.3. Preparation of FSM-based active edible films

FSM powder-carboxymethyl cellulose (CMC) blank blends were prepared by dissolving 1 % w/v of mucilage powder, 0.4 % w/v of carboxymethyl cellulose, and 0.4 % w/v of glycerol as a plasticizer in distilled water. Films were produced by casting on glass Petri dishes (6 cm diameter) and kept in the plane to ensure the homogeneous thickness of the films. The blank blend is defined as FSM/CMC. The active antimicrobial blends were manufactured by adding different concentrations of rosemary (REO) (1 %, 2 %, and 3 % v/v) to the FSM/CMC solution. Due to the very low solubility of REO in water, tween 80 (0.1 %, 0.2 %, and 0.3 % v/v) was added with REO at a volume ratio of 1:10 to the blend solution and then homogenized at 12000 rpm for 3 min. The solutions were centrifuged at 8000 rpm for 3 min to eliminate bubbles. The resulting solutions were poured onto Petri dishes and left to dry at room temperature and relative humidity (RH) of 38 ± 3 % for 24 h. The active biofilms are coded as FSM/CMC/REO 1 %, FSM/CMC/REO 2 %, and FSM/CMC/REO 3 %.

2.4. Characterization

2.4.1. Attenuated total reflectance Fourier-transform infrared spectroscopy (ATR-FTIR)

FT-IR spectra of the films were acquired using an FT-IR-4600 spectrometer (JASCO International Co. Ltd., Japan) equipped with a single crystal diamond Pro One ATR accessory. The samples were kept in a desiccator containing silica gel to remove the films' residual moisture and minimize the interference in the spectrum before the analyses. The spectra were measured by acquiring 32 scans from 400 to 4000 cm^{-1}, with a resolution of 4 cm^{-1} per scan.

2.4.2. Thermal gravimetric analysis (TGA)

The change in weight of the film samples was recorded via a thermogravimetric device (SDT- Q600, TA Instruments CO., USA). Samples were heated from 25 to 1000 °C at a controlled heating rate of 10 °C/min within a N_2 atmosphere.

2.4.3. Structural and morphological analysis of the films

The morphological properties and surface characteristics of the prepared samples were studied by scanning electron microscopy (SEM) (MIRA3, Tescan, Czech Republic) and atomic force microscopy (AFM) (Easyscan 2, Nanosurf, Switzerland) devices.

2.4.4. Tensile test

A universal material testing machine (STM-50, Santam, Tehran, Iran) was used to evaluate the mechanical characteristics of the prepared films. The films were cut into 1 × 5 cm^2 strips and stretched at a rate of 50 mm/min. 4 specimens were tested for each film, and the mean values were reported.

2.4.5. Thickness, moisture content, and water solubility of films

The film thickness was determined by a digital micrometer (Mitutoyo Corp. MDC-1 SB) with a precision of 0.001 mm. >10 random locations of the film were measured to compute the average film thickness, which is required to calculate the water vapor permeability and tensile features. The films' moisture content was assessed based on the methodology outlined by Zhang [23] with some modifications. The prepared samples (1 × 3 cm^2) were first weighed and then located in an oven at 105 °C for one day until reaching a constant weight. The moisture content was calculated using Eq. (1).

$$\mathrm{MC}\ (\%) = \frac{m_i - m_f}{m_i} \times 100 \tag{1}$$

MC represents the moisture content, m_i represents the sample's initial weight, and m_f shows its final weight.

To determine the water solubility, the prepared samples (1 × 3 cm^2) were subjected to a 24 h drying period in an oven set at 105 °C, and then their respective weights (m_i) were measured. Next, the dried samples were submerged in 30 mL distilled water (25 °C) for one day. The film residues that did not dissolve were separated by centrifugation at 3000 rpm for 15 min, followed by drying in an oven maintained at 105 °C for one day, and subsequent weight measurement (m_f). The solubility percentage in water (S%) was calculated according to Eq. (2) [24].

$$\mathrm{S}\% = \frac{m_i - m_f}{m_i} \times 100 \tag{2}$$

2.4.6. Water vapor permeability (WVP)

The WVP of the films was evaluated using the ASTM E96–95 method, with some modifications [25]. Circular glass cups with an entrance surface area of 0.0032 m^2 were filled with dry calcium chloride (RH of 0 %) and sealed by film samples. The cups were then positioned inside a desiccator with a controlled environment set at 75 % RH in the presence of a saturated sodium chloride solution. The water vapor transfer rate was assessed by regularly measuring the incremental change in the weight of the cup over 24 h. The WVP of the prepared samples was calculated as the mean of 3 replications using Eq. (3):

$$\mathrm{WVP} = \frac{w \times X}{A \times t \times \Delta P} \tag{3}$$

where w represents the water weight permitted through the sample (g), X represents the film thickness (mm), A refers to the entrance surface area of the cup (m^2), t indicates the penetration time (h), and ΔP stands for the difference in water vapor pressure existing between the opposing sides of the film (kPa) [26].

2.4.7. Color measurements

The color of the films was evaluated using a colorimeter (Minolta CR 400, Minolta Camera Co. Ltd., Japan). Film color was assessed by positioning it on a standard white screen. The measurements were conducted at 6 random sections of the films with 3 repetitions. Lightness (L) values vary from 0 (black) to 100 (white). Chromaticity parameters a and b range from −80 (green) to 100 (red) and − 80 (blue) to 70 (yellow), respectively. The color difference (ΔE) was measured using Eq. (4).

$$\sqrt{(L^* - L)^2 + (a^* - a)^2 + (b^* - b)^2} \tag{4}$$

where L* = 89.75, a* = 0.03, and b* = 1.83 indicate the color parameter amounts used to describe the standard white background, and L, a, and b exhibit the color parameter values of the samples [27].

2.4.8. Light transmission and transparency

The optical characteristics of the samples were evaluated via a UV–vis spectrophotometer (TU-1901, Beijing Purkinje General Instrument Co., China). The films were cut into precise sections and positioned within the test cell of the spectrophotometer, ensuring they were aligned perpendicular to the direction of the light beam. The transparency (T) of the films was calculated based on the Beer-Lambert law using Eq. (5).

$$\mathrm{T}\% = 10^{-A}X \times 100 \tag{5}$$

where A represents the absorbance recorded at a wavelength of 600 nm, and X shows the thickness of the film in mm [14].

2.5. Bioassay

2.5.1. Total phenol measurement

The quantification of phenol content in the films followed the procedure outlined by Chaovanalikit [28]. Briefly, 250 μL of the aqueous film solutions (8.33 mg/mL) were combined with 250 μL of 10 % Folin Ciocalteu reagent in a round-bottom test tube that contained 3.75 mL of distilled water. The obtained solution was agitated using a vortex for 10 s and left in the dark at room temperature for 10 min. After adding 750 μL of sodium carbonate (20 % w/v) to the solution, it was incubated for 20 min at 40 °C in a water bath. Lastly, the reaction was concluded by promptly cooling the sample in an ice bath. The absorbance of each sample was assessed at a wavelength of 765 nm using a UV–vis spectrophotometer. The results were stated as mg gallic acid equivalents per gram of dried film (GAE mg/g), following Eq. (6).

$$\mathrm{T} = \frac{\mathrm{C} \times \mathrm{V}}{\mathrm{M}} \tag{6}$$

where T represents the total phenolic content (GAE mg/g dried film), C denotes the concentration of gallic acid derived from the standard calibration curve (mg/mL), V represents the volume of the film extract (mL), and M signifies the weight of dried film (g).

2.5.2. Antibacterial activity of the films

A suitable diffusion method was employed to investigate the antibacterial properties of the prepared edible films. Gram-negative

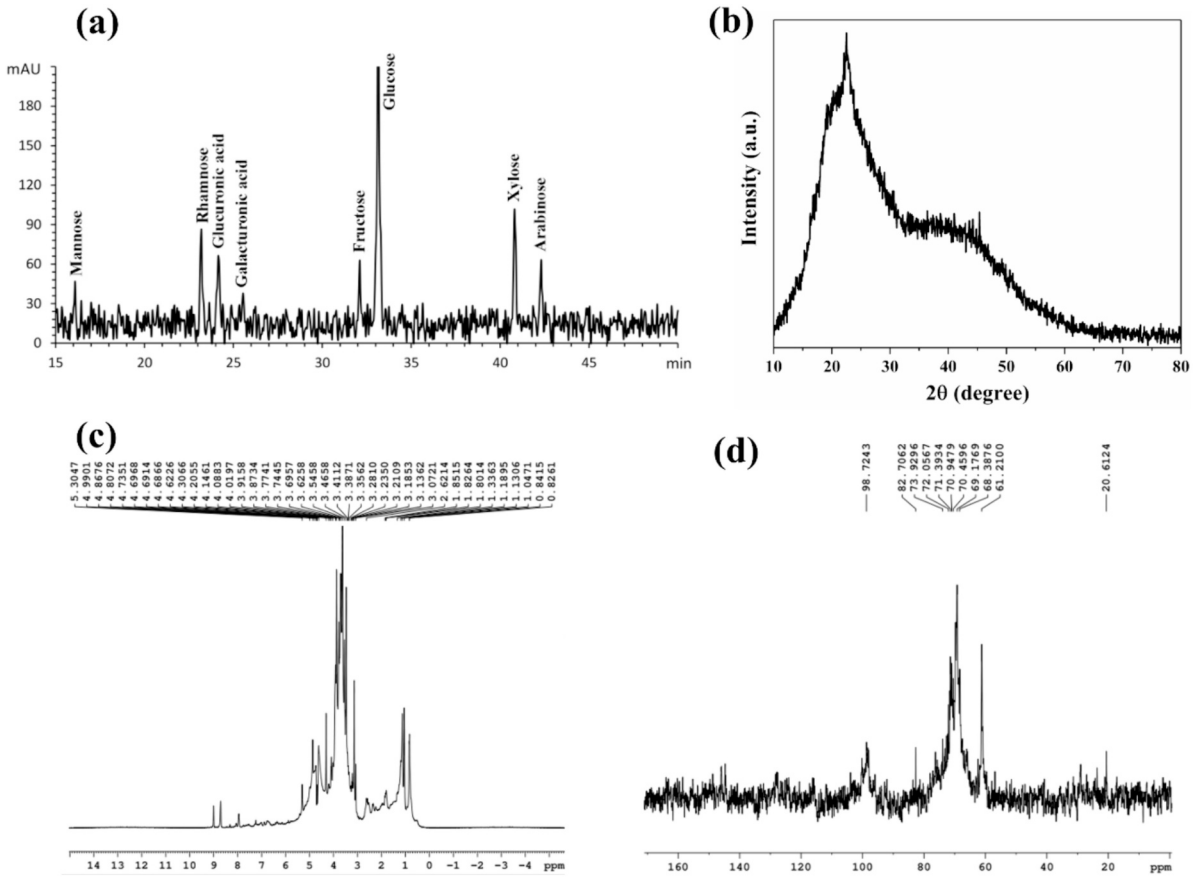

Fig. 1. (a) HPLC chromatogram, (b) XRD spectra, (c) ^{1}HNMR spectra, and (d) ^{13}CNMR spectra of the extracted FSM.

(*Escherichia coli*) and Gram-positive (*Staphylococcus aureus*) bacteria were studied, as representative of common food pathogens. The bacteria were first revived in a nutrient broth culture medium to conduct this test, and turbidity was adjusted to 0.5 McFarland. After that, the bacterial suspension was inoculated into NA plates and placed in an incubator at 37 °C for one day. Next, the film solutions were poured into the hole created in the middle of the NA plates; then, they were incubated for another 24 h at 37 °C [29,30]. The antibacterial activity was evaluated by quantifying the diameter (mm) of the inhibitory zone surrounding the well.

2.6. Applicability of the prepared films for fruit preservation

The effect of the prepared films for fruit preservation was investigated using apple as a model fruit. Whole apples were immersed in the solutions of control film and films containing 1 %, 2 %, and 3 % of REO, then were dried at room temperature. Their visual appearance was regularly assessed through observation for 30 days at ambient temperature and atmosphere.

2.7. Statistical analysis

All the experimental data underwent statistical analysis utilizing the SPSS software (Version 21, SPSS Inc., Chicago, USA). Analysis of variance (ANOVA) was observed data, followed by Tukey's multiple comparison test to discover significant differences ($p < 0.05$) in mean values from film analysis.

3. Results and discussion

3.1. Characterization of FSM

HPLC analysis was used to determine the monosaccharide composition of FSM, and the results are shown in Fig. 1a. Fenugreek seeds can show significant variability in their composition depending on the specific subspecies and the environmental conditions in which they are grown [31]. Hasaroeih et al. reported a high level of diversity among the ecotypes based on the measured characters, including antioxidant activity (48.19 to 86.85 %), phenol (0.82 to 1.51 mg gallic acid per g dry weight), flavonoid (1.07 to 3.11 mg quercetin per g dry weight), trigonelline (0.02 to 0.08 mmol/l), 4-hydroxyisoleucine (0.197 to 0.906 mg/g), sucrose (0.13 to 3.77 mM), glucose (1.07 to 12.1 mM), and fructose (13.3 to 45.5 mM) [32]. Besides, the method used to extract the mucilage can also influence the final composition [33,34]. The extraction method applied in this work resulted in the extraction of glucose (50.01 %), xylose (11.06 %), and rhamnose (9.42 %) as the main components. The other minor components were fructose, arabinose, glucuronic acid, mannose, and galacturonic acid. A similar method, used by Ashooriyan et al. for the extraction of *Plantago ovata* seed mucilage, showed similar extracted components in the mucilage (xylose (72.31 %), arabinose (16.08 %), rhamnose (2.65 %), galacturonic acid (2.35 %), glucose (2.56 %), galactose (2.21 %), and fucose (1.81 %)) [35].

X-ray diffraction is a principal technique for categorizing hydrocolloids into crystalline, non-crystalline (amorphous), and semi-crystalline structures. Sharp peaks indicate regular atomic and molecular arrangements characteristic of crystalline structures, whereas non-crystalline or amorphous structures produce broad halos. The X-ray diffraction spectrum of the FSM powder is shown in Fig. 1b. A main peak at 2Θ values of about 22° was noted, along with a broad halo at about

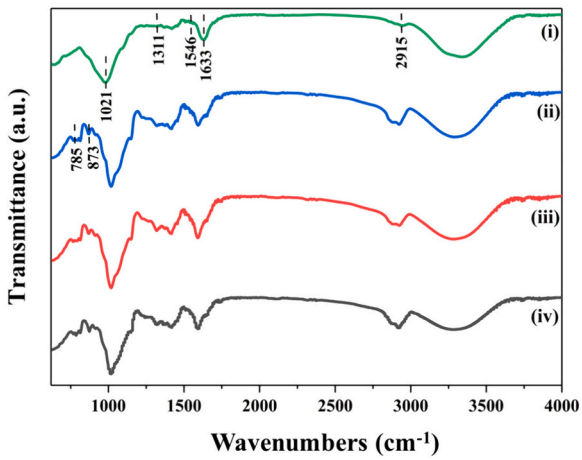

Fig. 2. FT-IR spectra of FSM/CMC films incorporated with different amounts of REO: (i) control, (ii) 1, (iii) 2, and (iv) 3 % (v/v).

40°. The presence of a broad peak at 2Θ values of about 22° has been previously reported for different polysaccharides and their derivatives, including hemicellulose xylan and cellulose [22,36,37]. The low intensity of the peak indicates poor crystallinity in the structure of the extracted fenugreek seed [38]. Similar results were reported for basil seed mucilage, *Plantago ovata* seed mucilage, and guar gum [35,39,40]. Amorphous polymers' transparency and good gas barrier properties make them great candidates as food packaging materials [41].

The results of NMR analysis of FSM are shown in Fig. 1c and d. The peaks appearing in the ^{1}H NMR spectrum at 5.304 and 4.306 ppm are related to -R-CHO- and -CH_2O-, respectively. These peaks also appeared in ^{13}C NMR spectra at 69.7 ppm for CHO and 61.21 ppm for CH_2O [42]. In the ^{1}H spectrum, the peaks crowded at the narrow area of 3 to 5 ppm indicate the existence of sugar residues [43]. The peak at 63 ppm in the ^{13}C spectrum and 4.146 and 6.622 ppm in the ^{1}H spectrum correspond to unbranched mannose, while the peaks at 387.68 ppm in the ^{13}C spectrum and 4.306 and 4.62 ppm in the ^{1}H spectrum are ascribed to branched C_6 [44]. The closely adjacent signals observed in the ^{1}H spectrum of mucilage (4.15 and 3.84 ppm) is related to H-1 of α-glucose, while the 3.55 to 3.39 ppm peaks are attributable to the OH and CH_2 groups of arabinoses. Furthermore, signals in the 3.1 to 4.1 ppm range can be ascribed to non-anomeric protons (H_2–H_6) [45].

3.2. Characterization of the active edible films

3.2.1. FT-IR spectroscopy of the films

FT-IR spectra of the FSM/CMC and FSM/CMC/REO films are shown in Fig. 2. The broad absorption peak in the range of 3100–3600 cm^{-1} is related to the stretching vibrations of the hydroxyl (O—H) groups [46]. For the FSM/CMC film, the characteristic bands at 1311, 1633, 1546, and 2915 cm^{-1} are consistent with the amide III (C—N and N—H stretching), amide II (N—H bending), amide I (C═O stretching), and aliphatic C—H in CH_3 groups, respectively [2]. The peak at 1021 cm^{-1} was ascribed to the hydroxyl group of glycerol [47].

In the FT-IR spectrum of REO, a peak at 2857–2925 cm^{-1} is due to an aliphatic C—H stretch in the oil. A broad peak between 3300 and 3500 cm^{-1} might be due to REO hydroxyl groups; the C═O stretching is observed at 1741 cm^{-1}, and the C—O absorption of terpenoid components is observed at 1021 cm^{-1} [48].

In the films containing 1, 2, and 3 % essential oil, a shift of -OH peak to higher frequencies from 3280 cm^{-1} to 3345 cm^{-1} and a shift in carboxyl group might be a result of the physical interaction by hydrogen bonding between REO with hydroxyl group matrices [49,50]. Besides, two peaks at 785 and 873 cm^{-1}, associated with the C—H out-of-plane bending vibrations of isoprenoids, confirm the inclusion of the essential oil in the polymer matrix [51].

3.2.2. Thermal analysis

The influence of essential oil on the thermal behavior of mucilage-based films was investigated by TGA and its first derivative (DTG) analyses. During the thermal degradation of polysaccharides, two phenomena typically occur. In the first stage, the removal of bonded and unbonded water molecules (dehydration) occurs, characterized by a slight weight loss of up to 200 °C [52]. In the second stage, breakage and dissociation of hydrocarbon chains occur, leading to significant weight loss and the formation of volatile products [53]. As depicted in Fig. 3a, for the control film and the film containing 3 % essential oil, 7.9 %, and 5.7 % weight loss occurred, respectively, in the temperature range of 24 to 160 °C, which is ascribed to the removal of water and volatile substances from the film [54]. The decreased weight loss for REO-bearing films compared to the control indicates their higher hydrophobicity, supported by the moisture content and water solubility results. The main loss mass between 160 and 341 °C is associated with several processes, including the thermal breakdown of specific polymers with low molecular weight in the film matrix, the evaporation of glycerol, and the decomposition of polysaccharide chains [53]. In this stage, the most significant weight loss was observed for the film containing 3 % REO (61.17 %). As can also be seen in the DTG curve, the films' thermal endurance was decreased with increasing essential oil content, which

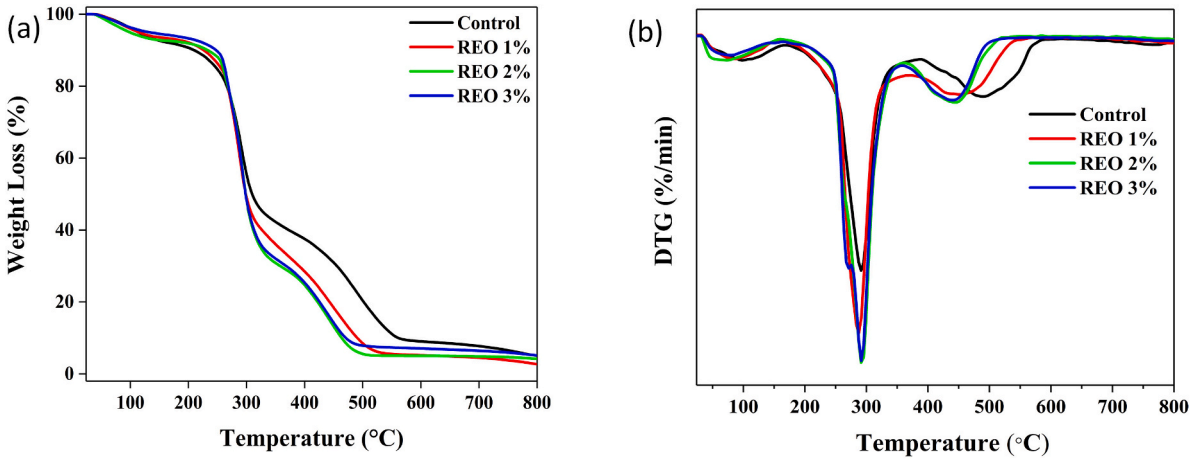

Fig. 3. (a) TGA and (b) DTG analyses of FSM/CMC control film and films containing different concentrations of REO.

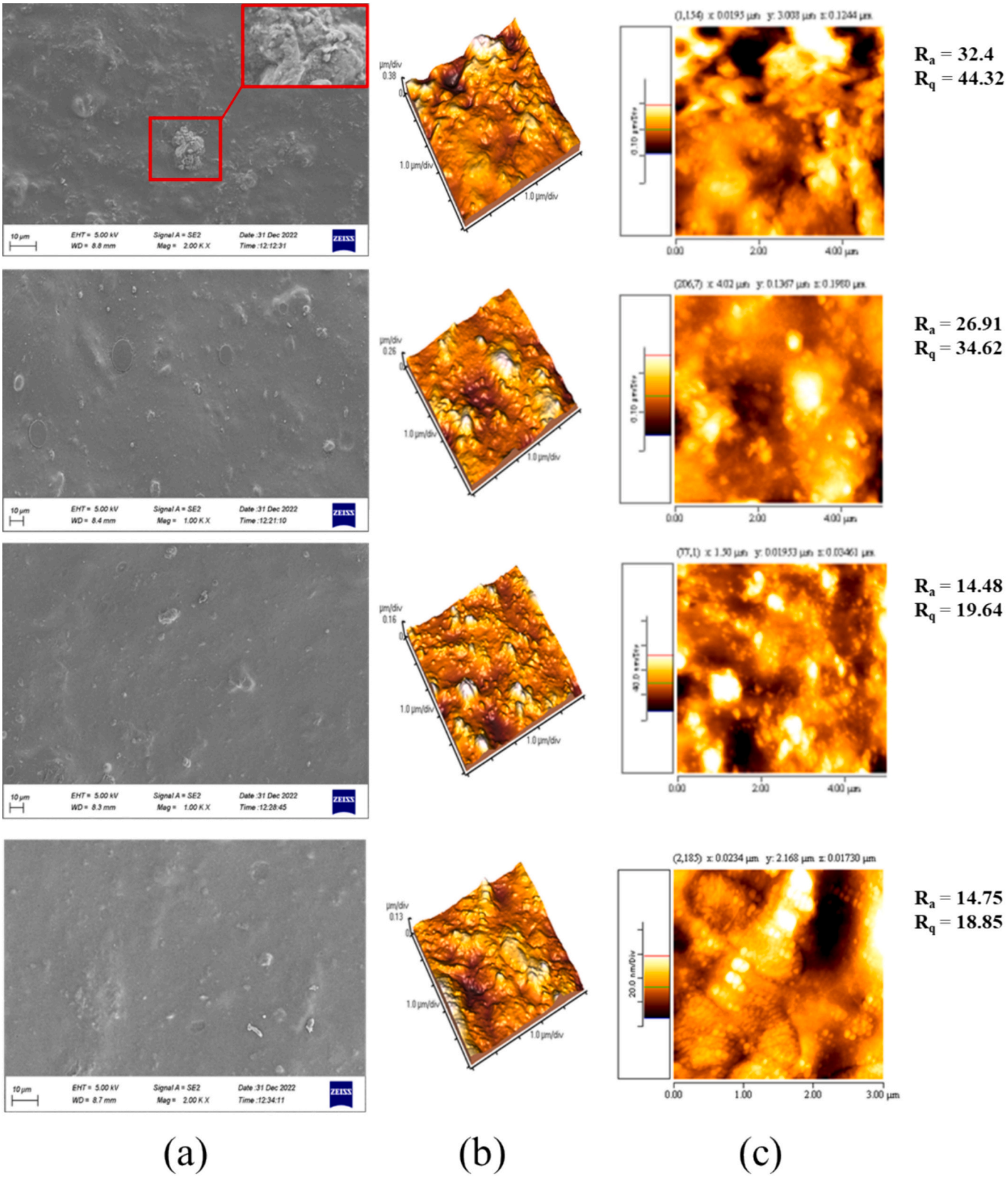

Fig. 4. (a) SEM, (b) AFM 3D surface topography, and (c) AFM 2D surface morphology images of the prepared films containing different REO concentrations.

was attributed to the interaction between the essential oil and the film matrix, causing a discontinuity in the film structure [55]. The intensity of the DTG peaks, as illustrated in Fig. 3b, displayed a direct correlation with the rate of weight alterations that occurred in the TGA thermographic profiles.

3.2.3. *Active edible film morphology*

To better understand the films' morphology, the biofilm microstructures were investigated using both SEM and AFM. The SEM morphographs are presented in Fig. 4a. The smooth and homogeneous surface without cracks or fractures of FSM/CMC film demonstrated

Table 1
Tensile strength (TS) and elongation at break (EB) values of FSM/CMC and FSM/CMC/REO biofilms.

Film	EB (%)	TS (MPa)
FSM/CMC	7.21 ± 0.11[a]	58.69 ± 3.40[a]
FSM/CMC/REO 1 %	6.93 ± 0.15[a]	36.71 ± 4.56[b]
FSM/CMC/REO 2 %	6.31 ± 0.24[b]	21.09 ± 2.45[c]
FSM/CMC/REO 3 %	4.97 ± 0.22[c]	15.41 ± 4.16[c]

[a-c]Different letters within a column indicate a significant difference ($p < 0.05$).

Table 2
Physicochemical properties of the films incorporated with different concentrations of REO.

Film	Moisture content (%)	Solubility in water (%)	WVP $\times 10^{-12}$ (g/s.m.Pa)	Thickness (mm)
FSM/CMC	22.98 ± 0.41[a]	29.8 ± 0.24[a]	0.55 ± 0.06[d]	0.03 ± 0.002[c]
FSM/CMC/REO 1 %	21.96 ± 0.33[a]	25.77 ± 0.28[b]	0.73 ± 0.04[c]	0.04 ± 0.004[b]
FSM/CMC/REO 2 %	18.56 ± 0.36[b]	23.07 ± 0.39[c]	1.43 ± 0.06[a]	0.05 ± 0.005[b]
FSM/CMC/REO 3 %	13.93 ± 0.45[c]	22.86 ± 0.35[c]	1.08 ± 0.05[b]	0.07 ± 0.004[a]

Values are presented as means ± standard deviation. [a-d]Different letters within a column indicate a significant difference ($p < 0.05$).

excellent compatibility of the components and good film-forming ability, which resulted from the interaction of FSM, CMC, and plasticizer during gelatinization [56]. Interestingly, the formulated film containing REO showed a smoother surface with a uniform essential oil distribution. The even dispersion of REO within the film might be attributed to the emulsifying influence of Tween 80, which could inhibit the segregation of REO droplets [57].

AFM analysis was executed to thoroughly examine the films' morphology and surface characteristics. Fig. 4b and c represents the films' 3D surface topography and 2D surface morphology, respectively. The FSM/CMC film exhibited a slightly irregular surface with roughness height, root-mean-square roughness (R_q), and average roughness (R_a) values of 312 nm, 44.32 nm, and 32.43 nm, respectively. For FSM/CMC/REO films, the roughness height, Rq, and Ra values decreased to 112 nm, 14.75 nm, and 18.85 nm, respectively, indicating a decrement in the films' surface roughness. These findings align with the study by Hosseini [2] on edible films incorporating *Origanum vulgare* L. essential oil. They explained that the liquid state of essential oil might cause the spread of lipophilic droplets of essential oil across the film surface upon drying, which filled the irregularities present on the film surface and made it smoother.

3.2.4. Mechanical properties

The mechanical strength of an edible film is a significant property for protecting the integrity of the food packaging during distribution and consumption. Elongation at break (EB) and tensile strength (TS) values of the prepared samples are displayed in Table 1. TS of the control film significantly decreased after the addition of REO, and the lowest TS (15.41 ± 4.16 MPa) was observed for the film containing 3 % REO. Essential oil partially replaced the strong polymer-polymer interactions in the film network with a weaker polymer-essential oil interaction [54]. Consequently, this process weakens the network structure, leading to a reduction in the TS of the films [26]. N. Mohsenabadi et al. also observed such changes in the TS for starch and CMC films containing different concentrations of REO [16]. EB of the films loaded by 2 and 3 % REO significantly decreased compared to the control film. The control film had an EAB of 7.21 ± 0.11 %, which reduced to 4.97 ± 0.22 % for the film containing 3 % essential oil. This can be explained by the discontinuity in the polymer matrix and changes in the polymer chain interactions in the presence of essential oil, leading to a mechanical response weakness [58]. Nonetheless, the active films still maintained ductility values compatible with their possible use as edible coatings.

3.2.5. Moisture content and film thickness

The moisture content of the films is shown in Table 2. The incorporation of REO into the films resulted in a reduction in their moisture content, from 22.98 ± 0.41 % for the control film to 13.93 ± 0.45 % for FSM/CMC/REO 3 %. This result is related to the hydrophobic nature of the essential oil, which decreased the hydrophilic sites for absorption of water molecules and the interaction between REO and polymer matrices [26]. Reduced moisture content has the potential to enhance film water resistance, inhibit microorganism proliferation, and consequently extend product shelf life [59].

The thickness of the control film (0.030 ± 0.002 mm) increased by increasing the essential oil concentration and reached 0.070 ± 0.004 mm for films containing 3 % essential oil, which could mainly be related to the more significant amount of solid content in the film-forming solutions. The thickness enhancement can be assigned to the entrapment and accumulation of REO droplets in the blend film [60]. The increase in thickness can potentially reduce the migration of solutes, thereby contributing to product quality and safety preservation.

3.2.6. Solubility in water

The capacity to resist water or to remain insoluble is vital for considering biofilms in food packaging, particularly in environments with elevated humidity levels [57]. Table 2 presents the water solubility characteristics of the films, which decreased as REO concentration increased ($p < 0.05$). The solubility percentage of the control film was 29.8 ± 0.24 %, while the FSM/CMC/REO 3 % solubility reduced to 22.86 ± 0.35 %. The incorporation of REO enhanced the water resistance of the films, which could be ascribed to the reduction in the hydrophilicity of the film resulting from the incorporation of the hydrophobic REO. In addition, the interaction between REO and the hydroxyl moieties of the polysaccharides led to a diminished affinity of the hydroxyl groups for water molecules, resulting in lower solubility [57,61]. A similar result was reported by M. Abadi et al., where increasing concentrations of REO in CMC-based films caused cross-linking in the film matrix, reducing the film affinity to water and their solubility [16].

3.2.7. Water vapor permeability (WVP)

Mass transfer between food and its surrounding environment can cause physicochemical changes or chemical reactions, leading to a decline in food quality. So, preventing or reducing the water exchange between the wrapped product and its medium is necessary [2,61]. As shown in Table 2, all prepared films demonstrated limited water vapor permeability (WVP). The control film exhibited the lowest WVP value ($0.55 \pm 0.06 \times 10^{-12}$ g/m.s.Pa), a metric that underwent augmentation following the incorporation of REO. Notably, the film containing 2 % (*v*/v) essential oil displayed the highest susceptibility to water vapor permeation, as indicated by its elevated WVP value ($1.43 \pm 0.06 \times 10^{-12}$ g/m.s.Pa) ($P < 0.05$). No visible difference was seen in the WVP of films when 2 % and 3 % essential oil were loaded. The increased WVP can be ascribed to the reduction of cohesion in the film and the creation of discontinuities owing to the existence of hydrophobic essential oil, leading to increased mass transport through the film [26,61]. Similarly, Zhou et al. reported enhancement in WVP of cassava starch/cinnamon essential oil films with an increment in essential oil concentration [57]. The elevated WVP levels of the films were attributed to the adverse influence of cinnamon essential oil on the microstructure of the films.

Table 3
Effect of different concentrations of REO on color parameters of FSM/CMC films.

Film	L*	a*	b*	C*	ΔE
Control	92.83 ± 0.67[a]	−1.44 ± 0.02[a]	11.02 ± 0.64[c]	11.11 ± 0.54[c]	13.02 ± 0.49[c]
FSM/CMC/REO 1 %	90.65 ± 0.59[b]	−1.95 ± 0.03[b]	15.3 ± 0.53[b]	15.46 ± 0.41[b]	17.15 ± 0.61[b]
FSM/CMC/REO 2 %	90.38 ± 0.86[b]	−2.09 ± 0.02[c]	16.09 ± 0.41[b]	16.23 ± 0.43[b]	17.77 ± 0.31[b]
FSM/CMC/REO 3 %	82.71 ± 0.92[c]	−2.58 ± 0.04[d]	23.83 ± 0.72[c]	23.84 ± 0.39[a]	26.42 ± 0.44[a]

Values are presented as means ± standard deviation. [a-d]Different letters within a column indicate a significant difference ($p < 0.05$).

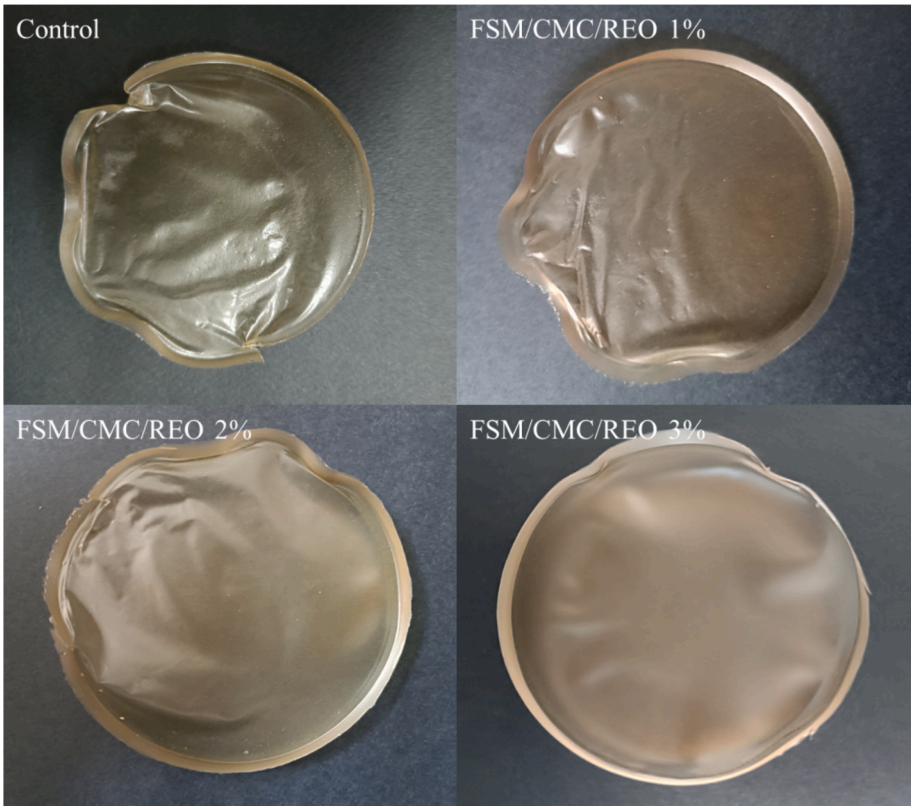

Fig. 5. Appearance of the FSM/CMC films with various REO concentrations.

This impact included the formation of micro-sized pores and openings within the film structure, which ultimately improved the mass transfer rate. The WVP amounts acquired in this study are notably lower in comparison to those previously reported for quince seed mucilage-based films incorporating thyme essential oil (14.91×10^{-11} g/s.m.Pa) [62], κ-carrageenan films containing *Satureja hortensis* essential oil (0.556×10^{-10} g/s.m.Pa) [63], and cassava starch-based films containing cinnamon essential oil (1.9×10^{-10} g/s.m.Pa) [57], further supporting their use in food packaging.

3.2.8. Colorimetric properties

The film's color impacts the visual presentation of packaged goods and their reception by consumers. The effect of REO concentrations on color values and total color difference are shown in Table 3, and the appearance of the prepared films is illustrated in Fig. 5. The color transparency of the films diminished with the elevation of essential oil concentration. Increasing the amount of REO caused a reduction in the brightness (L*) and greenness (a*) of the samples. Still, it increased their yellowness (b*), color intensity (C*), and total color difference (ΔE). Comparable findings were obtained for chitosan and starch films incorporating pomegranate peel extract and thyme essential oil [64].

3.2.9. Light transmission and transparency

The optical transparency of edible films holds significant importance because it can directly impact the visual quality of the coated product. The transmission of UV–visible light between 200 and 800 nm of the

Table 4
Light transmission and transparency of FSM/CMC films with different amounts of REO.

Film	Light transmission at different wavelengths (%)								Transparency*
	200	280	350	400	500	600	700	800	
FSM/CMC	0.01	0.03	2.11	21.85	53.1	61.39	65.18	67.63	7.06 ± 0.32[c]
FSM/CMC/REO 1 %	0	0.01	1.16	11.31	38.21	47.94	53.9	54.94	7.98 ± 0.26[b]
FSM/CMC/REO 2 %	0	0	0.11	10.78	37.35	46.99	53.5	58.21	8.19 ± 0.40[b]
FSM/CMC/REO 3 %	0	0	0.3	5.1	18.15	23.32	27.11	31.16	9.03 ± 0.32[c]

* [a-d]Different letters within a column indicate a significant difference ($p < 0.05$).

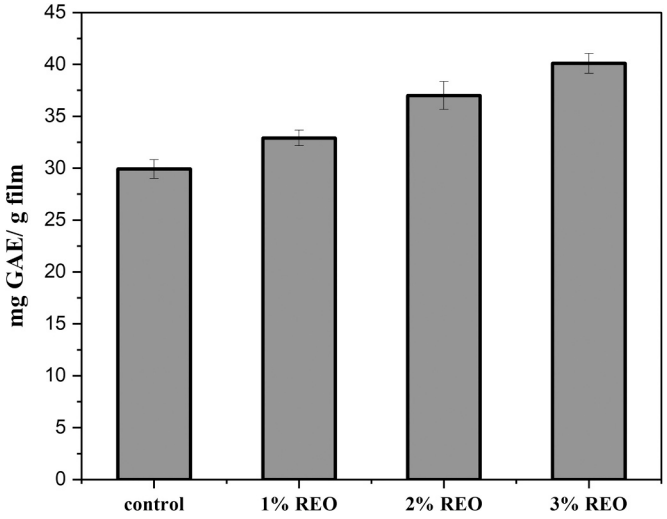

Fig. 6. Total phenolic content of FSM/CMC films containing different concentrations of REO.

Table 5
Antibacterial activity of FSM/CMC films incorporated different amounts of REO.

Film	Inhibition zone (mm)	
	S. aureus	*E. coli*
FSM/CMC	0	0
FSM/CMC/REO 1 %	13.22 ± 0.17^{c}	13.55 ± 0.52^{b}
FSM/CMC/REO 2 %	13.75 ± 0.21^{b}	13.98 ± 0.25^{b}
FSM/CMC/REO 3 %	14.31 ± 0.14^{a}	14.92 ± 0.33^{a}

[a-c]Different letters within a column indicate a significant difference ($p < 0.05$).

films containing different amounts of REO is reported in Table 4. Under UV irradiation between 200 and 280 nm, all samples displayed excellent absorption properties. However, in the visible light range, the films containing REO exhibited enhanced light transmission barrier properties compared to the control film. This decrease in light transmission is probably due to light scattering at the interfaces of the essential oil droplets loaded in the polymer matrix [2].

REO-loaded films exhibited lower transparency than the control film. The decrease in the transparency of edible films was associated with reduced light transmission because of the addition of essential oils. By increasing the REO concentration, the intensity of light scattering increased, resulting in the opaque appearance of the films [65,66].

3.2.10. Total phenolic content

The capacity of essential oils to neutralize free radicals through their antioxidant activity is mainly caused by their phenolic compounds. As shown in Fig. 6, the phenolic content of the control film was 29.92 ± 0.9 mg GAE/g dried film, which increased with increasing the concentration of REO and reached 40.1 ± 0.95 mg GAE/g dried film in the films incorporated with 3 % essential oil. The potent antioxidant properties of REO are associated with the active compounds, such as rosmarinic acid, carnosic acid, and carnosol, as well as monoterpenes, including 1,8-cineole, camphor, and α-pinene [20].

3.2.11. Antibacterial activity

The antibacterial activity of the films containing various concentrations of REO against Gram-negative bacterium *E. coli* and Gram-positive bacterium *S. aureus* are presented in Table 5. Most of the studies on the effect of essential oil against foodborne pathogens reported that they are slightly more active against Gram-positive bacteria than Gram-negative ones [67,68]. This phenomenon arises because of an outer membrane in Gram-negative bacteria, which provides a hydrophilic surface for the bacteria that acts as a barrier against penetration of macromolecules and hydrophobic substances. However, the outer membrane does not demonstrate absolute impermeability to hydrophobic molecules, and when the compound passes through it, it exerts antibacterial activity [69]. As shown in Fig. 7, the control film revealed no antibacterial properties.

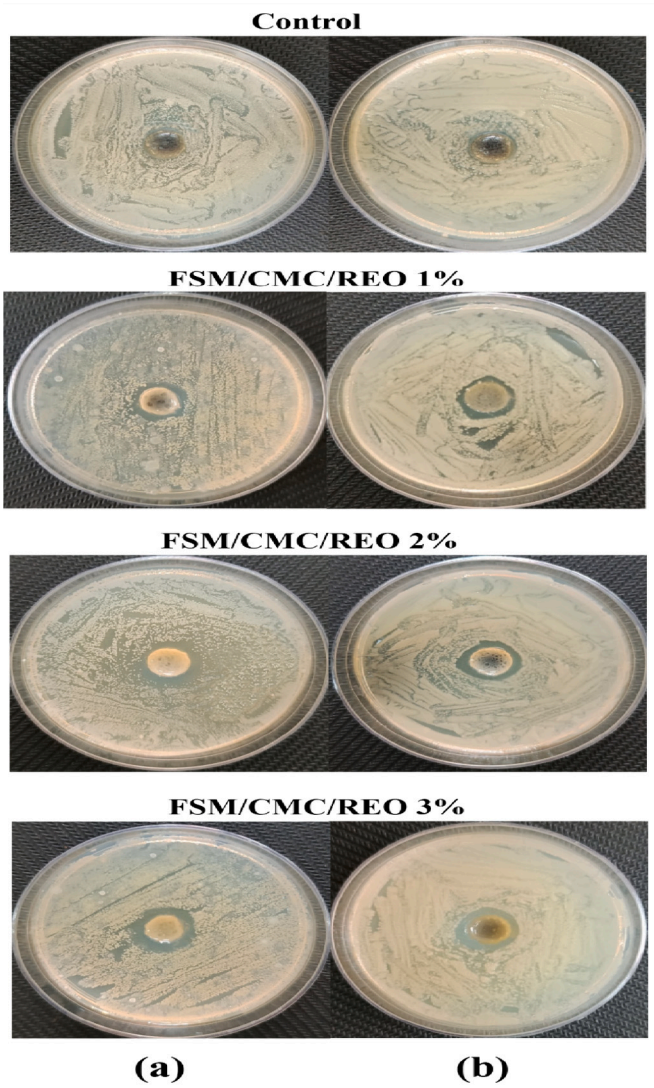

Fig. 7. Representative pictures of inhibitory zones of FSM/CMC films incorporated with different concentrations of REO against (a) *S. aureus* and (b) *E. coli*.

In contrast, the REO films showed antibacterial activity against *E. coli* and *S. aureus*, as revealed by the inhibitory zone formed around the wells. Furthermore, with the increase of REO concentrations, the diameter of the inhibitory zone increased. This result was due to phenolic compounds, including 1,8-cineole, α-pinene, and camphor, which have lipophilic and hydrophobic functional groups [20,70]. Essential oils' hydrophobic nature allows them to penetrate the lipids in bacterial cell membranes and mitochondria, causing membrane degradation and increasing [71].

3.2.12. Effect of edible film on fruit shelf life

The impact of the prepared samples on extending the fruit shelf life was investigated using apple as a model fruit. Fig. 8 shows photographs of uncoated and coated apples for 30 days of storage. As can be seen, the uncoated apple appears darker, and wrinkles develop on the skin. The apple dipped in the control film solution also changed slightly in color.

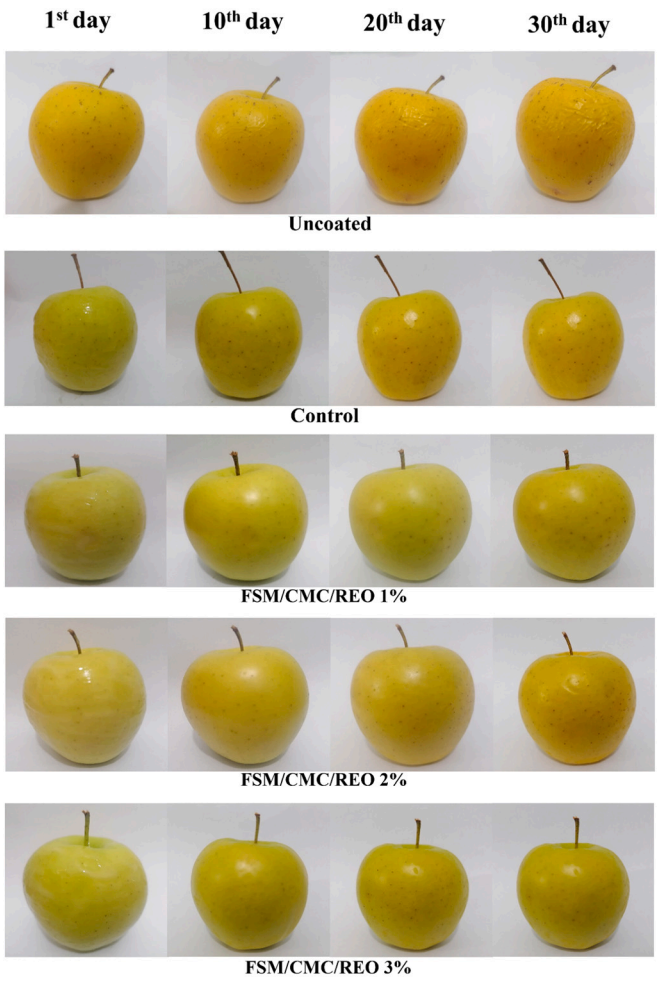

Fig. 8. Appearance of uncoated apples and apples covered with control film and films containing REO within 30 days.

However, the fruits dipped in the REO-containing films remained almost unchanged over the 30-day storage period. This suggests that these films effectively protected apples from deterioration by retarding dehydration and possibly by inhibiting microbial growth or slowing down the oxidation process that leads to spoilage.

4. Conclusions

In this study, native fenugreek seed mucilage (FSM) was extracted and characterized by HPLC, XRD, ^{1}H, and ^{13}C NMR. The composition of FSM monosaccharides includes glucose (50.01 %), xylose (11.06 %), and rhamnose (9.42 %). FSM-based active edible films were produced, including carboxymethyl cellulose (CMC) and different concentrations of rosemary essential oil (REO) (1–3 % v/v) as an active agent to prolong the shelf life of fruit. The interaction of REO with the polymer matrices caused peak shifts and alterations in intensity in FTIR, as well as modifying the thermal degradation of the films. SEM and AFM morphography revealed a uniform distribution of REO and smoother surfaces in the loaded films. Moreover, solubility tests indicated decreased water solubility with increased REO concentration from 1 % to 3 %. Similarly, the antimicrobial activity against *Staphylococcus aureus* and *Escherichia coli* and the antioxidant activity of REO-loaded biofilms escalated with the rising REO content. As a proof of concept, whole apples were used to verify the effectiveness of our coating, and the shelf-life assessment of dip-coated apples in all biofilm solutions indicated that the REO-loaded biofilms effectively extended the shelf life of apples to 30 days. These findings confirm that FSM extract is suitable for developing active, sustainable edible coating materials. However, further studies on sensorial aspects and antimicrobial activity evaluation on a larger number of microorganisms, including yeasts or molds, are needed. In addition, practical applications of the designed biofilms for food packaging are required to enhance the strength and applicability of our findings.

CRediT authorship contribution statement

Ali Mohammadi Lindi: Writing – original draft, Validation, Methodology, Investigation, Formal analysis, Data curation, Conceptualization. **Leila Gorgani:** Writing – original draft. **Maedeh Mohammadi:** Writing – review & editing, Supervision, Resources. **Sepideh Hamedi:** Writing – review & editing. **Ghasem Najafpour Darzi:** Resources. **Pierfrancesco Cerruti:** Writing – review & editing. **Ehsan Fattahi:** Writing – review & editing. **Arash Moeini:** Writing – review & editing, Writing – original draft, Validation, Supervision.

Declaration of competing interest

The authors declare that they have no known competing financial interests or personal relationships that could have appeared to influence the work reported in this paper.

Acknowledgment

This study was supported by Babol Noshirvani University of Technology, Iran, through a graduate research grant [BNUT/984115049/1402]. The European Union's Horizon 2020 research and innovation program (PRIMA call) partially funded the current work under grant agreement No. 02WPM1683, EU Project, “From Edible Sprouts to hEalthy food -FEED”.

References

[1] Z.J. Zhang, N. Li, H.Z. Li, X.J. Li, J.M. Cao, G.P. Zhang, D.L. He, Preparation and characterization of biocomposite chitosan film containing Perilla frutescens (L.) Britt. essential oil, Ind. Crop. Prod. 112 (2018) 660–667, https://doi.org/10.1016/J.INDCROP.2017.12.073.

[2] S.F. Hosseini, M. Rezaei, M. Zandi, F. Farahmandghavi, Bio-based composite edible films containing Origanum vulgare L. essential oil, Ind. Crop. Prod. 67 (2015) 403–413, https://doi.org/10.1016/J.INDCROP.2015.01.062.

[3] A. Moeini, P. Pedram, E. Fattahi, P. Cerruti, G. Santagata, Edible polymers and secondary bioactive compounds for food packaging applications: antimicrobial, mechanical, and gas barrier properties, Polymers (Basel) 14 (2022) 2395.

[4] M. Hoque, S. Gupta, R. Santhosh, I. Syed, P. Sarkar, Biopolymer-based edible films and coatings for food applications, in: Food, Medical, and Environmental Applications of Polysaccharides, 2021, pp. 81–107, https://doi.org/10.1016/B978-0-12-819239-9.00013-0.

[5] R. Kumar, S. Patil, M.B. Patil, S.R. Patil, M.S. Paschapur, Isolation and evaluation of disintegrant properties of fenugreek seed mucilage, Int. J. Pharmtech Res. 1 (2009) 982–996.

[6] A. Kumar, R.R. Kumar, V. Chaturvedi, A.M. Kayastha, α-Amylase purified and characterized from fenugreek (Trigonella foenum-graecum) showed substantial anti-biofilm activity against Staphylococcus aureus MTCC740, Int. J. Biol. Macromol. 252 (2023) 126442, https://doi.org/10.1016/j.ijbiomac.2023.126442.

[7] R. Aruna, B. Manjula, M. Penchalaraju, C. CHandrika, Effect of fenugreek seed mucilage on physico-chemical properties of Mosambi fruit juice, J. Pharmacogn. Phytochem. 7 (2018) 1887–1890.

[8] S.A. Wani, P. Kumar, Fenugreek: a review on its nutraceutical properties and utilization in various food products, J. Saudi Soc. Agric. Sci. 17 (2018) 97–106, https://doi.org/10.1016/J.JSSAS.2016.01.007.

[9] B.A. Behbahani, A.A. Imani Fooladi, Shirazi balangu (Lallemantia royleana) seed mucilage: chemical composition, molecular weight, biological activity and its evaluation as edible coating on beefs, Int. J. Biol. Macromol. 114 (2018) 882–889, https://doi.org/10.1016/J.IJBIOMAC.2018.03.177.

[10] A. Araújo, A. Galvão, C.S. Filho, F. Mendes, M. Oliveira, F. Barbosa, M.S. Filho, M. Bastos, Okra mucilage and corn starch bio-based film to be applied in food, Polym. Test. 71 (2018) 352–361, https://doi.org/10.1016/J.POLYMERTESTING.2018.09.010.

[11] S. Amiri, F. Nabizadeh, L. Rezazad Bari, A novel source of food hydrocolloids from Trigonella elliptica seeds: extraction of mucilage and comprehensive characterization, J. Sci. Food Agric. 102 (2022) 7144–7154.

[12] A.M. Mohite, D. Chandel, Formulation of edible films from fenugreek mucilage and taro starch, SN Appl. Sci. 2 (2020) 1–9.
[13] X. Hu, Y. Liu, D. Zhu, Y. Jin, H. Jin, L. Sheng, Preparation and characterization of edible carboxymethyl cellulose films containing natural antibacterial agents: lysozyme, Food Chem. 385 (2022) 132708, https://doi.org/10.1016/J.FOODCHEM.2022.132708.
[14] X. Li, Z. Ren, R. Wang, L. Liu, J. Zhang, F. Ma, M.Z.H. Khan, D. Zhao, X. Liu, Characterization and antibacterial activity of edible films based on carboxymethyl cellulose, Dioscorea opposita mucilage, glycerol and ZnO nanoparticles, Food Chem. 349 (2021) 129208, https://doi.org/10.1016/J.FOODCHEM.2021.129208.
[15] R. Avila-Sosa, E. Palou, A. López-Malo, Essential oils added to edible films, in: Essential Oils in Food Preservation, Flavor and Safety, 2016, pp. 149–154, https://doi.org/10.1016/B978-0-12-416641-7.00015-8.
[16] N. Mohsenabadi, A. Rajaei, M. Tabatabaei, A. Mohsenifar, Physical and antimicrobial properties of starch-carboxy methyl cellulose film containing rosemary essential oils encapsulated in chitosan nanogel, Int. J. Biol. Macromol. 112 (2018) 148–155, https://doi.org/10.1016/J.IJBIOMAC.2018.01.034.
[17] A. Moeini, N. Germann, M. Malinconico, G. Santagata, Formulation of secondary compounds as additives of biopolymer-based food packaging: a review, Trends Food Sci. Technol. 114 (2021) 342–354, https://doi.org/10.1016/j.tifs.2021.05.040.
[18] S. Falah, M. Ghorbani, M. Azimifar, Superamphiphilic polymeric coating in membrane application: a mini-review, Mini Rev. Org. Chem. 20 (2023) 438–454.
[19] F. Xue, Y. Gu, Y. Wang, C. Li, B. Adhikari, Encapsulation of essential oil in emulsion based edible films prepared by soy protein isolate-gum acacia conjugates, Food Hydrocoll. 96 (2019) 178–189, https://doi.org/10.1016/J.FOODHYD.2019.05.014.
[20] Z.A. Shektaei, M.M. Pourehsan, V. Bagheri, Z. Ghasempour, M. Mahmoudzadeh, A. Ehsani, Physico-chemical and antimicrobial characteristics of novel biodegradable films based on gellan and carboxymethyl cellulose containing rosemary essential oil, Int. J. Biol. Macromol. 234 (2023) 122944, https://doi.org/10.1016/J.IJBIOMAC.2022.12.163.
[21] M. Stramarkou, V. Oikonomopoulou, T. Missirli, I. Thanassoulia, M. Krokida, Encapsulation of rosemary essential oil into biodegradable polymers for application in crop management, J. Polym. Environ. 28 (2020) 2161–2177, https://doi.org/10.1007/S10924-020-01760-5/METRICS.
[22] A.M. Lindi, S. Falah, M. Sadeghnezhad, M. Ghorbani, Optimization of fenugreek seed mucilage extraction for the synthesis of a novel bio-nano composite for efficient removal of cadmium ions from aqueous environments, Int. J. Biol. Macromol. 261 (2024) 129882, https://doi.org/10.1016/j.ijbiomac.2024.129882.
[23] P. Zhang, Y. Zhao, Q. Shi, Characterization of a novel edible film based on gum ghatti: effect of plasticizer type and concentration, Carbohydr. Polym. 153 (2016) 345–355, https://doi.org/10.1016/J.CARBPOL.2016.07.082.
[24] R. Gheribi, L. Puchot, P. Verge, N. Jaoued-Grayaa, M. Mezni, Y. Habibi, K. Khwaldia, Development of plasticized edible films from Opuntia ficus-indica mucilage: a comparative study of various polyol plasticizers, Carbohydr. Polym. 190 (2018) 204–211, https://doi.org/10.1016/J.CARBPOL.2018.02.085.
[25] M. Beigomi, M. Mohsenzadeh, A. Salari, Characterization of a novel biodegradable edible film obtained from Dracocephalum moldavica seed mucilage, Int. J. Biol. Macromol. 108 (2018) 874–883, https://doi.org/10.1016/J.IJBIOMAC.2017.10.184.
[26] Z. Liu, D. Lin, R. Shen, R. Zhang, L. Liu, X. Yang, Konjac glucomannan-based edible films loaded with thyme essential oil: physical properties and antioxidant-antibacterial activities, Food Packag. Shelf Life 29 (2021) 100700, https://doi.org/10.1016/J.FPSL.2021.100700.
[27] R. Wang, X. Li, L. Liu, W. Chen, J. Bai, F. Ma, X. Liu, W. Kang, Preparation and characterization of edible films composed of Dioscorea opposita Thunb. mucilage and starch, Polym. Test. 90 (2020) 106708, https://doi.org/10.1016/J.POLYMERTESTING.2020.106708.
[28] A. Chaovanalikit, R.E. Wrolstad, Total anthocyanins and total phenolics of fresh and processed cherries and their antioxidant properties, J. Food Sci. 69 (2004) FCT67–FCT72, https://doi.org/10.1111/J.1365-2621.2004.TB17858.X.
[29] P. Kanmani, J.W. Rhim, Physicochemical properties of gelatin/silver nanoparticle antimicrobial composite films, Food Chem. 148 (2014) 162–169, https://doi.org/10.1016/J.FOODCHEM.2013.10.047.
[30] S. Falah, M. Ghorbani, J. Ahmadpour, Photocatalytic degradation of anionic and cationic dyes over PPy/CuFe2O4 nanocomposite under visible-light and bactericidal action, J. Taiwan Inst. Chem. Eng. 144 (2023) 104767, https://doi.org/10.1016/J.JTICE.2023.104767.
[31] K.M. McCormick, R.M. Norton, H.A. Eagles, Phenotypic variation within a fenugreek (*Trigonella foenum-graecum* L.) germplasm collection. II. Cultivar selection based on traits associated with seed yield, Genet. Resour. Crop. Evol. 56 (2009) 651–661.
[32] N.E. Hasaroeih, F. Ghanavati, F. Moradi, J.A. Kohpalkani, M. Rahimizadeh, Multivariate analysis of seed chemical diversity among wild fenugreek (Trigonella monantha CA Mey.) ecotypes, BMC Plant Biol. 23 (2023) 324.
[33] F. Rashid, S. Hussain, Z. Ahmed, Extraction purification and characterization of galactomannan from fenugreek for industrial utilization, Carbohydr. Polym. 180 (2018) 88–95.
[34] S.B. Dhull, P. Bamal, M. Kumar, S.P. Bangar, P. Chawla, A. Singh, W. Mushtaq, M. Ahmad, S. Sihag, Fenugreek (Trigonella foenum graecum) gum: a functional ingredient with promising properties and applications in food and pharmaceuticals—a review, Legume Sci. 5 (2023) e176.
[35] P. Ashooriyan, M. Mohammadi, G. Najafpour Darzi, M. Nikzad, Development of Plantago ovata seed mucilage and xanthan gum-based edible coating with prominent optical and barrier properties, Int. J. Biol. Macromol. 248 (2023) 125938, https://doi.org/10.1016/J.IJBIOMAC.2023.125938.
[36] R. Niknam, M. Mousavi, H. Kiani, New studies on the galactomannan extracted from Trigonella foenum-graecum (Fenugreek) seed: effect of subsequent use of ultrasound and microwave on the physicochemical and rheological properties, Food Bioprocess Technol. 13 (2020) 882–900.
[37] P.D. Cara, M. Pagliaro, A. Elmekawy, D.R. Brown, P. Verschuren, N.R. Shiju, G. Rothenberg, Hemicellulose hydrolysis catalysed by solid acids, Catal. Sci. Technol. 3 (2013) 2057–2061.
[38] F. Rashid, Z. Ahmed, S. Hussain, J.Y. Huang, A. Ahmad, Linum usitatissimum L. seeds: flax gum extraction, physicochemical and functional characterization, Carbohydr. Polym. 215 (2019) 29–38, https://doi.org/10.1016/J.CARBPOL.2019.03.054.
[39] S. Nazir, I.A. Wani, Fractionation and characterization of mucilage from Basil (Ocimum basilicum L.) seed, J. Appl. Res. Med. Aromat. Plants 31 (2022) 100429, https://doi.org/10.1016/J.JARMAP.2022.100429.
[40] P.L.R. Cunha, R.R. Castro, F.A.C. Rocha, R.C.M. De Paula, J.P.A. Feitosa, Low viscosity hydrogel of guar gum: preparation and physicochemical characterization, Int. J. Biol. Macromol. 37 (2005) 99–104, https://doi.org/10.1016/J.IJBIOMAC.2005.09.001.
[41] V. Siracusa, Food packaging permeability behaviour: a report, Int. J. Polym. Sci. 2012 (2012), https://doi.org/10.1155/2012/302029.
[42] E.D. Skakovskii, L.Y. Tychinskaya, V.A. Mauchanava, E.G. Karankevich, S. A. Lamotkin, A.D. Ahabalayeva, V.N. Reshetnikov, Combining nmr spectroscopy and gas-liquid chromatography for analysis of the fatty acid composition of fenugreek seed oil (Trigonella foenum graecum l.), J. Appl. Spectrosc. 80 (2013) 779–782, https://doi.org/10.1007/S10812-013-9842-0.
[43] A.K. Nayak, D. Pal, K. Santra, Screening of polysaccharides from tamarind, fenugreek and jackfruit seeds as pharmaceutical excipients, Int. J. Biol. Macromol. 79 (2015) 756–760, https://doi.org/10.1016/J.IJBIOMAC.2015.05.018.
[44] E. Ponzini, A. Natalello, F. Usai, M. Bechmann, F. Peri, N. Müller, R. Grandori, Structural characterization of aerogels derived from enzymatically oxidized galactomannans of fenugreek, sesbania and guar gums, Carbohydr. Polym. 207 (2019) 510–520, https://doi.org/10.1016/J.CARBPOL.2018.11.100.
[45] U.V. Deore, H.S. Mahajan, Isolation and characterization of natural polysaccharide from Cassia Obtustifolia seed mucilage as film forming material for drug delivery, Int. J. Biol. Macromol. 115 (2018) 1071–1078, https://doi.org/10.1016/J.IJBIOMAC.2018.04.174.
[46] S. Mayer, M. Tallawi, I. De Luca, A. Calarco, N. Reinhardt, L.A. Gray, K. Drechsler, A. Moeini, N. Germann, Antimicrobial and physicochemical characterization of 2,3-dialdehyde cellulose-based wound dressings systems, Carbohydr. Polym. 272 (2021) 118506, https://doi.org/10.1016/j.carbpol.2021.118506.
[47] M.S. Hoque, S. Benjakul, T. Prodpran, Effect of heat treatment of film-forming solution on the properties of film from cuttlefish (Sepia pharaonis) skin gelatin, J. Food Eng. 96 (2010) 66–73, https://doi.org/10.1016/J.JFOODENG.2009.06.046.
[48] A. Nowak, D. Kalemba, M. Piotrowska, A. Czyżowska, Effects of thyme (Thymus vulgaris L.) and rosemary (Rosmarinus officinalis L.) essential oils on growth of Brochothrix thermosphacta, Afr. J. Microbiol. Res. 7 (2013) 3396–3404.
[49] A. Moeini, P. Pedram, T. Goudoulas, T. Mehlhorn-Diehl, F. Gestmann, E. Fattahi, T. Becker, N. Germann, Encapsulation of Neem oil from Azadirachta indica into poly (lactic-co-glycolic acid) as a novel sprayable miticide system with long-term storage stability and controlled release kinetic, Ind. Crop. Prod. 201 (2023) 116954.
[50] A. Moeini, A. Cimmino, M. Masi, A. Evidente, A. Van Reenen, The incorporation and release of ungeremine, an antifungal Amaryllidaceae alkaloid, in poly (lactic acid)/poly (ethylene glycol) nanofibers, J. Appl. Polym. Sci. 137 (2020) 49098.
[51] C.M. Topala, L.D. Tataru, ATR-FTIR study of thyme and rosemary oils extracted by supercritical carbon dioxide, Rev. Chim. (Bucharest) 67 (2016) 842–846.
[52] A. Moeini, A. Cimmino, G. Dal Poggetto, M. Di Biase, A. Evidente, M. Masi, P. Lavermicocca, F. Valerio, A. Leone, G. Santagata, M. Malinconico, Effect of pH and TPP concentration on chemico-physical properties, release kinetics and antifungal activity of chitosan-TPP-Ungeremine microbeads, Carbohydr. Polym. 195 (2018) 631–641, https://doi.org/10.1016/j.carbpol.2018.05.005.
[53] T.L. Cao, K. Bin Song, Effects of gum karaya addition on the characteristics of loquat seed starch films containing oregano essential oil, Food Hydrocoll. 97 (2019) 105198, https://doi.org/10.1016/J.FOODHYD.2019.105198.
[54] A. Moeini, S. Mallardo, A. Cimmino, G. Dal Poggetto, M. Masi, M. Di Biase, A. van Reenen, P. Lavermicocca, F. Valerio, A. Evidente, M. Malinconico, G. Santagata, Thermoplastic starch and bioactive chitosan sub-microparticle biocomposites: antifungal and chemico-physical properties of the films, Carbohydr. Polym. 230 (2020) 115627, https://doi.org/10.1016/j.carbpol.2019.115627.
[55] N. Noshirvani, B. Ghanbarzadeh, C. Gardrat, M.R. Rezaei, M. Hashemi, C. Le Coz, V. Coma, Cinnamon and ginger essential oils to improve antifungal, physical and mechanical properties of chitosan-carboxymethyl cellulose films, Food Hydrocoll. 70 (2017) 36–45, https://doi.org/10.1016/J.FOODHYD.2017.03.015.
[56] R. Wang, X. Li, Z. Ren, S. Xie, Y. Wu, W. Chen, F. Ma, X. Liu, Characterization and antibacterial properties of biodegradable films based on CMC, mucilage from Dioscorea opposita Thunb. and Ag nanoparticles, Int. J. Biol. Macromol. 163 (2020) 2189–2198, https://doi.org/10.1016/J.IJBIOMAC.2020.09.115.
[57] Y. Zhou, X. Wu, J. Chen, J. He, Effects of cinnamon essential oil on the physical, mechanical, structural and thermal properties of cassava starch-based edible films, Int. J. Biol. Macromol. 184 (2021) 574–583, https://doi.org/10.1016/J.IJBIOMAC.2021.06.067.
[58] L. Sánchez-González, M. Cháfer, A. Chiralt, C. González-Martínez, Physical properties of edible chitosan films containing bergamot essential oil and their

inhibitory action on Penicillium italicum, Carbohydr. Polym. 82 (2010) 277–283, https://doi.org/10.1016/J.CARBPOL.2010.04.047.
[59] E. Díaz-Montes, R. Castro-Muñoz, Edible films and coatings as food-quality preservers: an overview, Foods 10 (2021) 249, https://doi.org/10.3390/FOODS10020249, 2021, Vol. 10, Page 249.
[60] Y. Lei, H. Wu, C. Jiao, Y. Jiang, R. Liu, D. Xiao, J. Lu, Z. Zhang, G. Shen, S. Li, Investigation of the structural and physical properties, antioxidant and antimicrobial activity of pectin-konjac glucomannan composite edible films incorporated with tea polyphenol, Food Hydrocoll. 94 (2019) 128–135, https://doi.org/10.1016/J.FOODHYD.2019.03.011.
[61] A. Dashipour, V. Razavilar, H. Hosseini, S. Shojaee-Aliabadi, J.B. German, K. Ghanati, M. Khakpour, R. Khaksar, Antioxidant and antimicrobial carboxymethyl cellulose films containing Zataria multiflora essential oil, Int. J. Biol. Macromol. 72 (2015) 606–613, https://doi.org/10.1016/J.IJBIOMAC.2014.09.006.
[62] M. Jouki, S.A. Mortazavi, F.T. Yazdi, A. Koocheki, Characterization of antioxidant–antibacterial quince seed mucilage films containing thyme essential oil, Carbohydr. Polym. 99 (2014) 537–546, https://doi.org/10.1016/J.CARBPOL.2013.08.077.
[63] S. Shojaee-Aliabadi, H. Hosseini, M.A. Mohammadifar, A. Mohammadi, M. Ghasemlou, S.M. Ojagh, S.M. Hosseini, R. Khaksar, Characterization of antioxidant-antimicrobial κ-carrageenan films containing Satureja hortensis essential oil, Int. J. Biol. Macromol. 52 (2013) 116–124, https://doi.org/10.1016/J.IJBIOMAC.2012.08.026.
[64] T. Mehdizadeh, H. Tajik, A.M. Langroodi, R. Molaei, A. Mahmoudian, Chitosan-starch film containing pomegranate peel extract and Thymus kotschyanus essential oil can prolong the shelf life of beef, Meat Sci. 163 (2020) 108073, https://doi.org/10.1016/J.MEATSCI.2020.108073.
[65] T.E. Swaty, Global refining industry trends: the present and future, Hydrocarb. Process. 84 (2005) 35–46.
[66] P. Tongnuanchan, S. Benjakul, T. Prodpran, Properties and antioxidant activity of fish skin gelatin film incorporated with citrus essential oils, Food Chem. 134 (2012) 1571–1579, https://doi.org/10.1016/J.FOODCHEM.2012.03.094.
[67] B. Bozin, N. Mimica-Dukic, I. Samojlik, E. Jovin, Antimicrobial and antioxidant properties of Rosemary and Sage (*Rosmarinus officinalis* L. and *Salvia officinalis* L., Lamiaceae) essential oils, J. Agric. Food Chem. 55 (2007) 7879–7885, https://doi.org/10.1021/JF0715323.
[68] M. Abdollahi, M. Rezaei, G. Farzi, Improvement of active chitosan film properties with rosemary essential oil for food packaging, Int. J. Food Sci. Technol. 47 (2012) 847–853, https://doi.org/10.1111/J.1365-2621.2011.02917.X.
[69] D. Sánchez Aldana, S. Andrade-Ochoa, C.N. Aguilar, J.C. Contreras-Esquivel, G. V. Nevárez-Moorillón, Antibacterial activity of pectic-based edible films incorporated with Mexican lime essential oil, Food Control 50 (2015) 907–912, https://doi.org/10.1016/J.FOODCONT.2014.10.044.
[70] M. Alizadeh Sani, A. Ehsani, M. Hashemi, Whey protein isolate/cellulose nanofibre/TiO2 nanoparticle/rosemary essential oil nanocomposite film: its effect on microbial and sensory quality of lamb meat and growth of common foodborne pathogenic bacteria during refrigeration, Int. J. Food Microbiol. 251 (2017) 8–14, https://doi.org/10.1016/J.IJFOODMICRO.2017.03.018.
[71] A. Bouyahya, J. Abrini, N. Dakka, Y. Bakri, Essential oils of Origanum compactum increase membrane permeability, disturb cell membrane integrity, and suppress quorum-sensing phenotype in bacteria, J. Pharm. Anal. 9 (2019) 301–311, https://doi.org/10.1016/J.JPHA.2019.03.001.